

Multifaceted yrast structure and the onset of deformation in $^{96,97}\text{Sr}$ and $^{98,99}\text{Zr}$

C. Y. Wu, H. Hua, D. Cline, A. B. Hayes, and R. Teng

Nuclear Structure Research Laboratory, Department of Physics, University of Rochester, Rochester, New York 14627, USA

R. M. Clark, P. Fallon, A. Goergen, A. O. Macchiavelli, and K. Vetter

Nuclear Science Division, Lawrence Berkeley National Laboratory, Berkeley, California 94720, USA

(Received 7 September 2004; published 14 December 2004)

Neutron-rich $^{96,97}\text{Sr}$ and $^{98,99}\text{Zr}$ nuclei were populated as fission fragments produced by the $^{238}\text{U}(\alpha, f)$ fusion-fission reaction. The yrast states of these nuclei have been extended up to $\approx 20\hbar$, which is about $6\hbar$ on average beyond the previously known spin, by studying the prompt γ rays in coincidence with the detection of both fission fragments. This extension allows the observation of yrast states with spins beyond $\approx 4^+$ in ^{96}Sr and ^{98}Zr evolving from vibrationlike states to rotationlike states. With an additional neutron, the yrast states with excitation energies above ≈ 600 keV in ^{97}Sr and ^{99}Zr have the characteristics of members of rotationlike bands for both positive- and negative-parity states. However, their underlying single-particle configurations cannot be determined uniquely by the measured intensity ratios of $\Delta I=1$ to $\Delta I=2$ transitions because of possible configuration mixing. The sharp variations in the yrast structure of these nuclei are discussed in terms of the gradualness of the onset of quadrupole deformation.

DOI: 10.1103/PhysRevC.70.064312

PACS number(s): 23.20.Lv, 25.70.Jj, 25.85.Ca, 27.60.+j

I. INTRODUCTION

One notable feature among many diverse phenomena of nuclear structure for neutron-rich $A \sim 100$ nuclei, where the valence nucleons begin to fill the $g_{9/2}$ proton and $h_{11/2}$ neutron orbitals, is the sudden onset of quadrupole deformation occurring in Sr and Zr isotopes with neutron number $N=60$. This can be understood within the framework of shape coexistence [1], where two shapes with very different deformation coexist in these nuclei and swap their relative locations between the ground and the excited states at ^{98}Sr and ^{100}Zr [2]. The absolute magnitude of their deformation and mixing has been the subject of many studies both experimentally and theoretically [3–10].

Strongly deformed excited states with quadrupole deformation of $0.35 < \beta_2 < 0.40$ coexisting with the nearly spherical ground states have been reported for Sr and Zr isotopes with neutron numbers $N=58$ and 59 [11–15]. This provides convincing evidence for the interpretation of the sudden onset of quadrupole deformation in terms of shape coexistence for nuclei in this mass region. However, the results were challenged by the recent measurement [16], which indicates that the well-defined strongly deformed excited configurations do not exist in these nuclei and the onset of quadrupole deformation is a gradual rather than a sudden process. This recent measurement was made by studying the γ -ray spectroscopy of $^{96,97}\text{Sr}$ and $^{98,99}\text{Zr}$, produced by spontaneous fission of ^{248}Cm , using the EUROAM2 array [17]. Medium spin levels of presumed deformed structures in these nuclei were identified using triple- γ coincidence data while their deformations were derived from the lifetimes of excited states, measured using the Doppler profile method (DPM) [18]. Deformations of $\beta_2=0.25(2)$ and $0.22(2)$ were found for the quasirotational structures with spins above 4^+ in ^{96}Sr and ^{98}Zr , respectively. Both positive- and negative-parity rotational bands with excitation energy above ≈ 600 keV were

identified in ^{97}Sr and ^{99}Zr , however the deformation was determined only for the negative-parity bands with $\beta_2=0.32(2)$ and $0.28(1)$, respectively.

The DPM is applicable for cases where the lifetimes of excited states in fission fragments are comparable to the stopping time of these fragments in the thick target-backing material, which typically is about 1–3 ps [16]. The disadvantage is that the resulting Doppler broadening of deexcited γ -ray transitions, when observed in a 4π detector array, limits the study to excited states having lifetimes longer than or comparable to the stopping time. In other words, it is an obstacle to observe higher-spin members of any given collective band because their lifetimes could be shorter than the stopping time, due to the increasing transition energy and rate. This shortcoming can be eliminated by using a thin target-backing material [19–21], which allows both fission

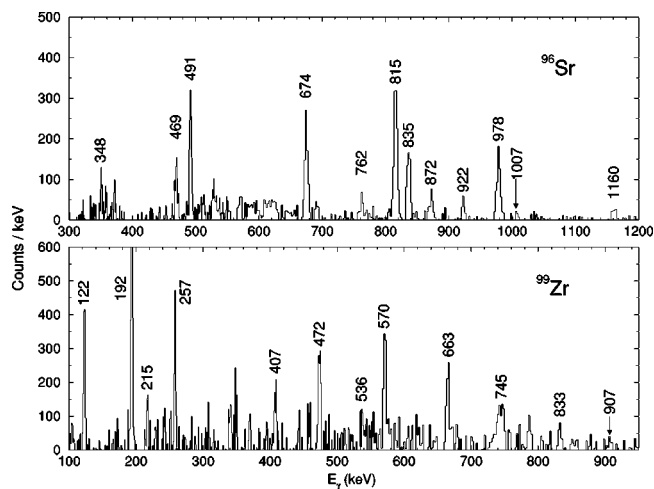


FIG. 1. Doppler-shift corrected prompt γ -ray spectrum derived from multiple double gates placed on prompt transitions in ^{96}Sr (top) and in ^{99}Zr (bottom).

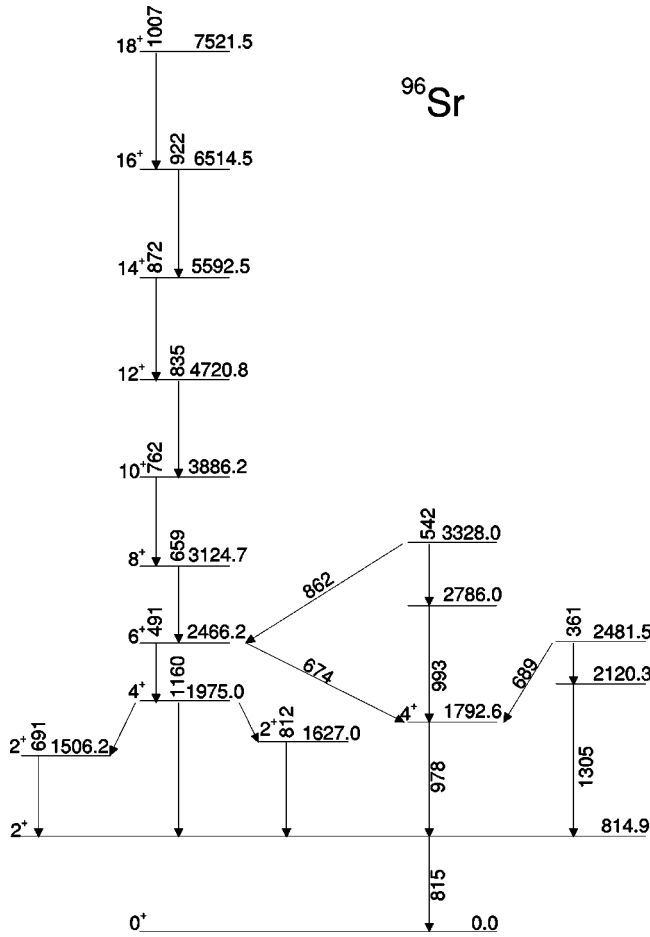


FIG. 2. Partial level scheme of ^{96}Sr with energies labeled in keV. The uncertainty on the transition energies is ≈ 1 keV.

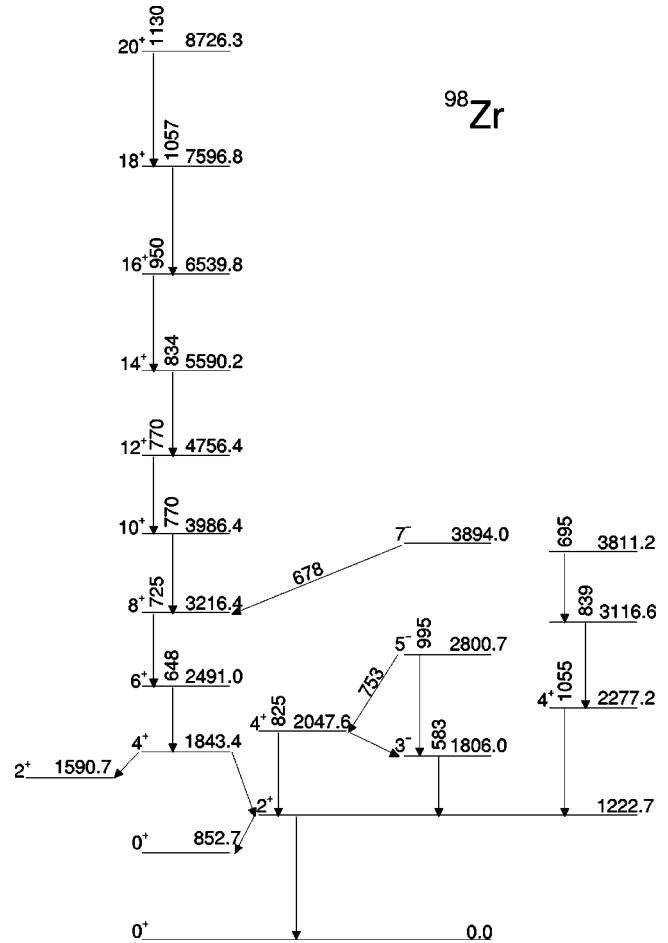


FIG. 3. Partial level scheme of ^{98}Zr with energies labeled in keV. The uncertainty on the transition energies is ≈ 1 keV.

fragments to recoil into the vacuum and to be detected in coincidence with the detection of deexcitation γ rays. Thus the Doppler shift of observed γ rays can be corrected according to the measured fission kinematics. The advantages of this thin-target technique have been recognized in the spectroscopy of neutron-rich Zr and Mo isotopes [22], where the yrast states have been extended up to $\approx 20\hbar$ compared to $\approx 14\hbar$ reached by the thick-target technique [23] even with an order of magnitude more statistics for the latter.

A similar advantage also is realized for $^{96,97}\text{Sr}$ and $^{98,99}\text{Zr}$ in our recent fusion-fission experiment with a thin target [22,24–26], where the yrast states were extended up to $\approx 20\hbar$. With such an opportunity to observe the higher-spin members of yrast structure for these nuclei, the systematics of the evolution of collective modes of motion can be studied in terms of not only spin but also the proton and neutron number in this rapidly shape-changing region. In this paper, the yrast structure and, in particular, the imprint of the gradualness of the onset of quadrupole deformation on the yrast structure are discussed.

II. EXPERIMENT

The present fusion-fission experiment was performed at the 88-in. cyclotron facility of the Lawrence Berkeley Na-

tional Laboratory. A $300 \mu\text{g}/\text{cm}^2$ ^{238}U target on an $\approx 30 \mu\text{g}/\text{cm}^2$ carbon backing was bombarded with an α beam at $E_{\text{lab}}=30$ MeV. Fission fragments were detected by the Rochester 4π , highly segmented heavy-ion detector ar-

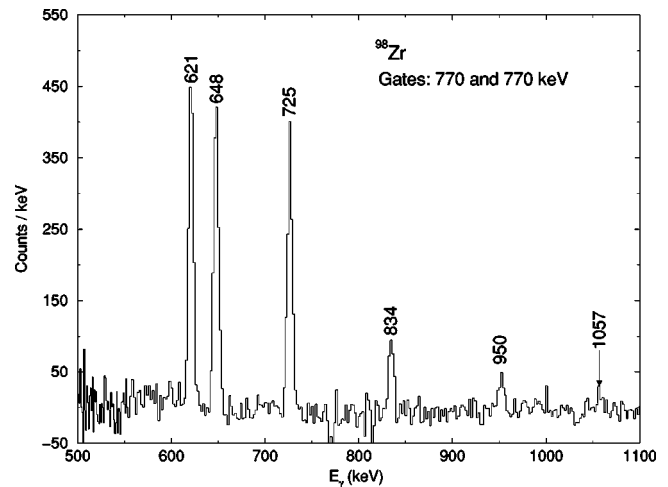


FIG. 4. Doppler-shift corrected prompt γ -ray spectrum derived from a double gate placed on the same prompt γ -ray energy, 770 keV, in ^{98}Zr .

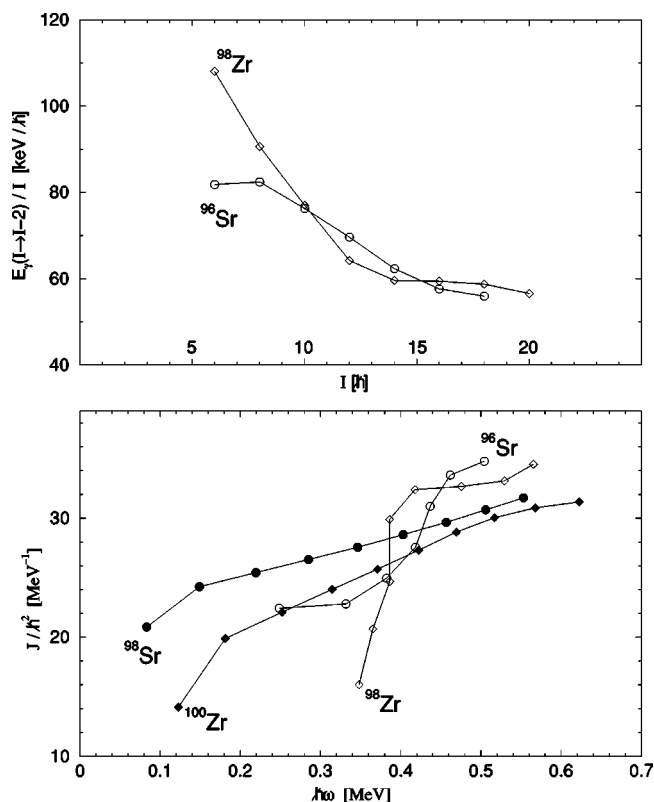


FIG. 5. Kinematic moment of inertia as a function of rotational frequency for the yrast states with spin above 4^+ in ^{96}Sr and ^{98}Zr and for the ground-state bands in ^{96}Sr and ^{100}Zr (bottom). The 911.3, 1010.3, and 1104.6 keV γ rays were assigned, for the first time, to the $14^+ \rightarrow 12^+$, $16^+ \rightarrow 14^+$, and $18^+ \rightarrow 16^+$ transitions, respectively, in ^{96}Sr from the present work. E-GOS plots for the yrast states in ^{96}Sr and ^{98}Zr (top).

ray, CHICO [21], in coincidence with the detection of deexcitation γ rays using Gammasphere. This particle detector has a geometric coverage for scattering angles from 12° to 85° and 95° to 168° relative to the beam axis and an azimuthal angle totaling 280° out of 360° . A valid event required the detection of both fission fragments and at least three coincident γ rays. Scattering angles of fission fragments and the time-of-flight difference between two fragments were recorded in addition to the γ -ray energies and coincident time. A total of $\approx 6 \times 10^8$ p-p- γ - γ events were collected.

Masses and velocity vectors of both fragments were deduced from the measured fission kinematics assuming the total kinetic energy is the same as that for ^{240}Pu spontaneous fission [27]. This assumption, that the prompt fission originates from the Pu-like compound nucleus, was supported by the observed γ -ray cross correlation between the partner fragment pairs. The deduced mass distribution of the fission fragments has a mass resolution about 12 mass units, which reflects the time resolution, ≈ 500 ps, plus the position resolution of $\approx 1^\circ$ in polar angle and 4.6° in azimuthal angle. The achieved resolutions are consistent with prior CHICO performance [19,28–33].

Mass-gated events with three or higher coincident γ rays were used to develop the level schemes of $^{96,97}\text{Sr}$ and $^{98,99}\text{Zr}$.

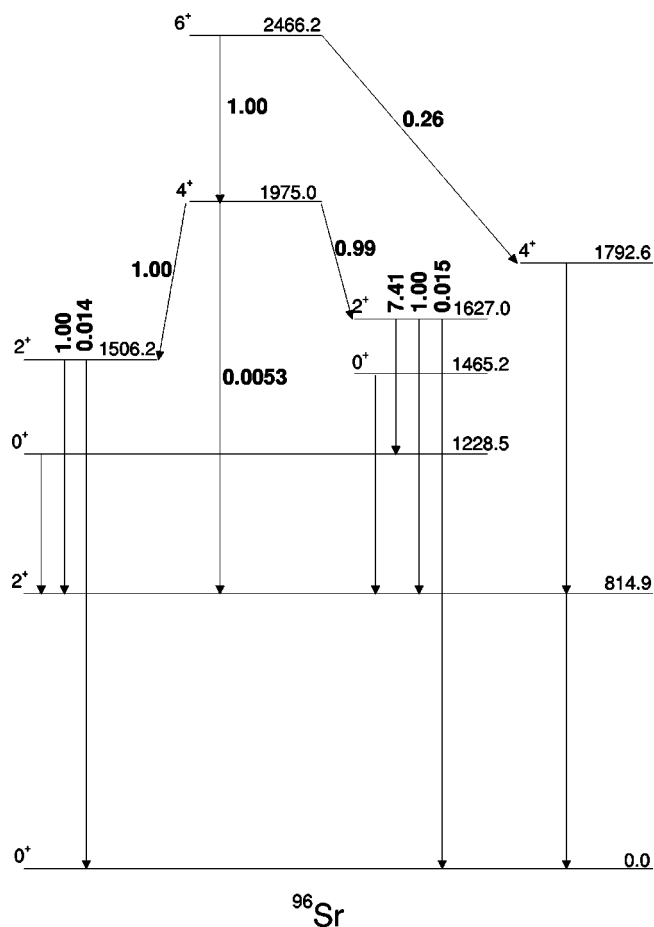


FIG. 6. Relative $B(E2)$ values in boldface for the low-lying states in ^{96}Sr derived from the present work. The data for the second and third 2^+ state are quoted from Ref. [36]. Excitation energies are in keV.

The added selectivity, provided by this mass gate, reduces the “background” γ rays of nuclei that are not of current interest, which enhances the ability to study nuclei produced with low yield or having weak transition strengths. Doppler-shift corrected γ -ray spectra, gated by the mass and the known γ -ray transitions in ^{96}Sr and ^{99}Zr , are shown in Fig. 1. The resulting energy resolution is better than 1%, limited primarily by the finite size of the Ge detector. Since the origin of γ rays from either fission fragment was established, after the proper Doppler-shift corrections were made, no sharp γ -ray transitions from the partner fragments are visible in these spectra. The resultant spectra are clean and straightforward to interpret.

III. RESULTS AND DISCUSSION

A. ^{96}Sr and ^{98}Zr

The spectroscopy of ^{96}Sr and ^{98}Zr , the $N=58$ isotones, has been studied extensively in the past and the most recent results [16,23] were obtained by experiments measuring high-fold γ -ray transitions for fission fragments produced by either ^{248}Cm or ^{252}Cf fission sources. Partial level schemes for these nuclei, deduced from the present work, are shown in

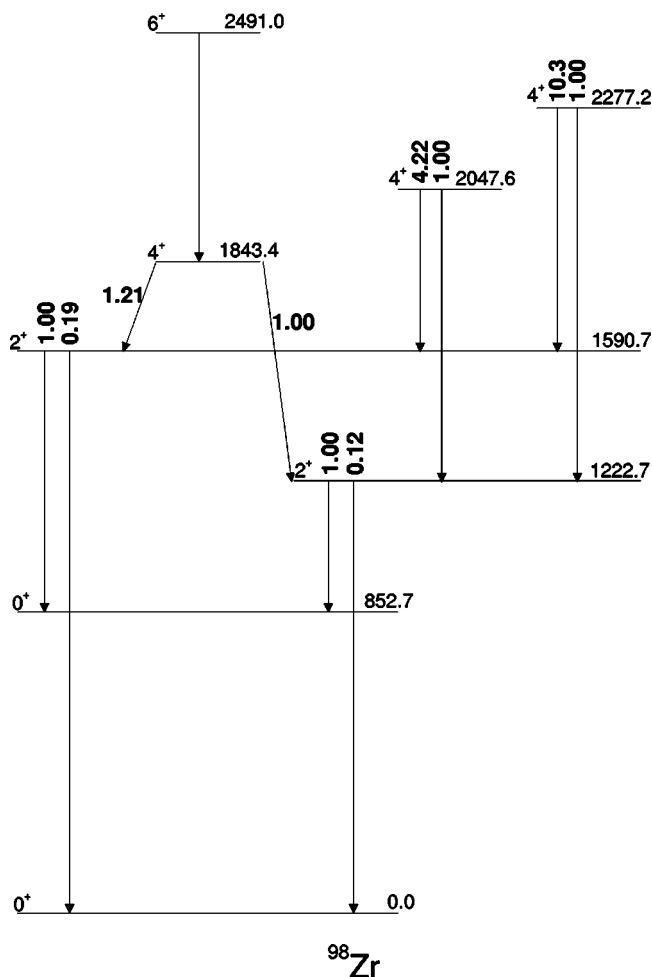


FIG. 7. Relative $B(E2)$ values in boldface for the low-lying states in ^{98}Zr derived from the present work. The data for the second 2^+ state and the second and third 4^+ state are quoted from Ref. [37]. Excitation energies are in keV.

Figs. 2 and 3 for ^{96}Sr and ^{98}Zr , respectively. Both level schemes are complicated except for the yrast states with spins above 4^+ , where the development of deformation or collective strength results in a noticeable band structure. The yrast states in ^{96}Sr have been extended from spin 12^+ to spin 18^+ at 7521.5 keV. The assigned $12^+ \rightarrow 10^+$ transition, 834.6 keV, is nearly 4 keV lower than 838.5 keV assigned earlier [16]. The difference is attributed to a broad distribution of this γ -ray transition for the latter [16] because the lifetime of the 12^+ state probably is comparable to the stopping time.

For ^{98}Zr , the yrast states have been extended from spin 16^+ to spin 20^+ at 8726.3 keV. However, the assigned γ -ray energies for both $14^+ \rightarrow 12^+$ and $16^+ \rightarrow 14^+$ transitions are systematically lower than those assigned earlier [23] by $\approx 1\text{--}2\text{eV}$. Presumably, it is the same complication encountered by the thick-target experiments, where an accurate determination of the transition energy is difficult for the excited state with the lifetime comparable to the stopping time. The proposed yrast sequence composed of γ rays, 834 - 770 - 770 - 725 keV, given in Ref. [23] is confirmed and illustrated in Fig. 4, where the feeding and the decay transitions, correlated by a double gate placed on the same

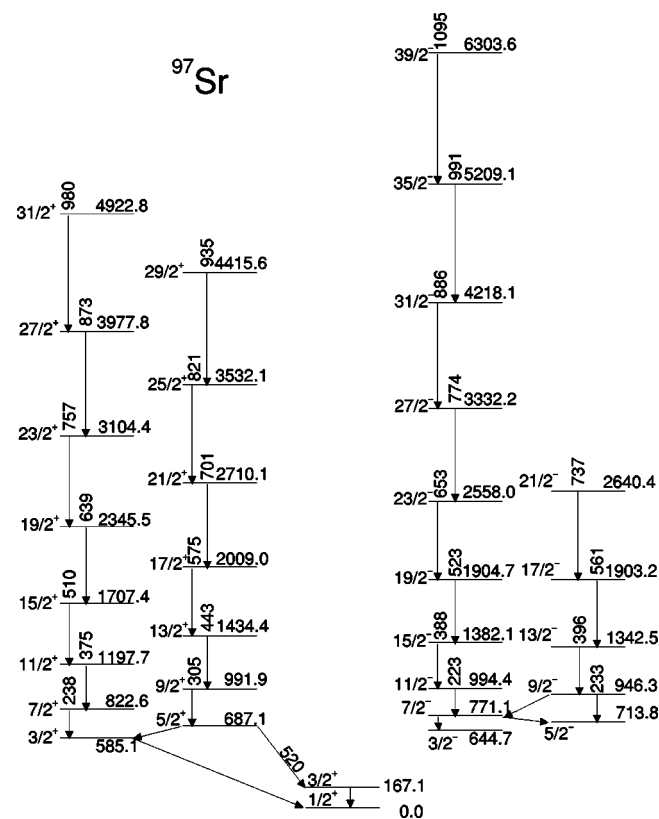


FIG. 8. Partial level scheme of ^{97}Sr with energies labeled in keV. The uncertainty on the transition energies is ≈ 1 keV.

770 keV γ ray, are shown. This is in disagreement with the results of Ref. [16].

The quadrupole deformation parameter, β_2 , increases from a value between 0.22 and 0.25 for the excited deformed structure of ^{96}Sr and ^{98}Zr [16] to a value between 0.32 and 0.35 for the ground state of ^{96}Sr and ^{100}Zr [34]. Note that for Ref. [16], the γ -ray energy is nearly 4 keV off the peak value for the $12^+ \rightarrow 10^+$ transition in ^{96}Sr and a questionable γ -ray decay sequence was used in ^{98}Zr . The influence of these discrepancies on the derived quadrupole deformation is unknown. The deformation difference between $N=58$ and $N=60$ isotones leaves the imprint illustrated in the lower part of Fig. 5, where the kinematic moment of inertia as a function of rotational frequency is plotted. In contrast to the well-defined rotational bands observed in ^{98}Sr and ^{100}Zr , the collective modes of motion in ^{96}Sr and ^{98}Zr have characteristics that range between vibration and rotation; that is, the moments of inertia have a vibrationlike character for the yrast states with spin up to 14^+ and then saturate at a value close to the rigid-rotor limit for states with spin above 14^+ . This transition happens at a rotational frequency close to the band crossing frequency ≈ 500 keV observed in ^{100}Zr [22]. This evolution from vibrational to rotational structure as a function of spin also is manifest in the upper part of Fig. 5, where the ratio of $E_\gamma(I \rightarrow I-2)/I$ versus spin I is plotted, that is, the so-called E-GOS (E-Gamma Over Spin) curve [35]. For a vibrator, the value of this ratio gradually diminishes to zero as the spin increases, while for an axially symmetric rotor it approaches a constant, $4(\hbar^2/2J)$.

TABLE I. Relative γ -ray intensities for transitions in $^{96,97}\text{Sr}$ and $^{98,99}\text{Zr}$. The statistical error is quoted for the measured relative intensity in this work and the systematic error could be up to 30% for the weak branches.

Transition	E_γ (keV)	Relative intensity	
		This work	Other work ^a
^{96}Sr			
$6_1^+ \rightarrow 4_1^+$	673.6	1.26(7)	1.42(14)
$6_1^+ \rightarrow 4_2^+$	491.2	1.00	1.00
$4_2^+ \rightarrow 2_1^+$	1160.1	0.50(3)	0.67(10)
$4_2^+ \rightarrow 2_2^+$	468.8	1.00	1.00
$4_2^+ \rightarrow 2_3^+$	348.0	0.22(4)	0.42(9)
^{97}Sr			
$9/2^- \rightarrow 7/2^-$	175.2	1.87(20)	0.80(51)
$9/2^- \rightarrow 5/2^-$	232.5	1.00	1.00
^{98}Zr			
$4_1^+ \rightarrow 2_1^+$	620.7	1.00	1.00
$4_1^+ \rightarrow 2_2^+$	252.7	0.014(2)	0.052(18)
$2_1^+ \rightarrow 0_1^+$	1222.7	1.00	1.00
$2_1^+ \rightarrow 0_2^+$	370.0	0.021(2)	0.009(3), 0.016(2) ^b
^{99}Zr			
$9/2^- \rightarrow 7/2^-$	188.5	1.43(9)	1.00(18), 1.64(49) ^c
$9/2^- \rightarrow 5/2^-$	199.7	1.00	1.00
$13/2^- \rightarrow 11/2^-$	457.9	0.38(3)	
$13/2^- \rightarrow 9/2^-$	411.6	1.00	
$7/2^+ \rightarrow 5/2^+$	215.0	0.73(5)	0.50(9)
$7/2^+ \rightarrow 3/2^+$	407.4	1.00	1.00
$9/2^+ \rightarrow 7/2^+$	256.6	0.65(4)	0.56(13)
$9/2^+ \rightarrow 5/2^+$	471.6	1.00	1.00

^aReference [16].

^bReference [37].

^cReference [15].

Another interesting observation is for the decay of excited states below the yrast 6^+ state. The relative $B(E2)$ values for these transitions are given in Figs. 6 and 7 for ^{96}Sr and ^{98}Zr , respectively. They are derived from the decay γ -ray branching ratios, which are determined, in turn, from the gated spectrum with the gates set on the appropriate feeding transitions and are listed in Table I together with those from other work. The 6^+ state at 2466.2 keV in ^{96}Sr decays to the first and second 4^+ states at 1792.6 and 1975.0 keV, respectively, with a relative $B(E2)$ strength of 0.26 to 1.00, which is an indication of mixing between these two 4^+ states. The 1792.6 keV 4^+ state decays mainly to the first 2^+ state at 814.9 keV while the 1975.0 keV 4^+ state decays to the second and third 2^+ states at 1506.2 and 1627.0 keV, respectively, with nearly identical $B(E2)$ strength. This could imply a $\approx 50/50$ mixing for the second and third 2^+ states. Their similar transition $B(E2)$ ratios to the ground state and the first 2^+ state are consistent with this mixing scenario. Note that the relative γ -ray branching ratio, given in Ref. [16], for the transition of the second 4^+ state to the third 2^+ state is nearly a factor of 2 higher than the present measurement.

Significant mixing between the first and second 2^+ states at 1222.7 and 1590.7 keV, respectively, in ^{98}Zr is suggested

based on their similar feeding and decay patterns. They are both fed by the first 4^+ state at 1843.4 keV with a $B(E2)$ strength $\approx 45\%$ of the total to the first 2^+ state and with the remaining strength to the second 2^+ state. This is consistent with their similar transition $B(E2)$ ratios to the ground state and the second 0^+ state at 852.7 keV. Note that the relative γ -ray branching ratio, given in Ref. [16], for the transition of the first 4^+ state to the second 2^+ state is nearly a factor of 4 higher than the present measurement [37].

Shape coexistence, particularly the excited deformed structure, in ^{96}Sr and ^{98}Zr has been discussed extensively in Ref. [16]. Contrary to the earlier finding [11,13] of the existence of strongly deformed excited 0^+ states, moderately deformed excited configurations were identified for the medium-spin yrast states by the work of Ref. [16]. It is still possible, however, that a strongly deformed excited 0^+ state coexists with a weakly deformed 0^+ (ground) state in these nuclei. The considerable softness of shape degrees of freedom, pointed out by the calculation of Ref. [38], may lead to a significant mixing between the excited 2^+ states of these two shapes. Note that the mixing for the weakly deformed shape happens to be a two-phonon state in ^{96}Sr and a one-phonon state in ^{98}Zr . A resulting moderately deformed shape

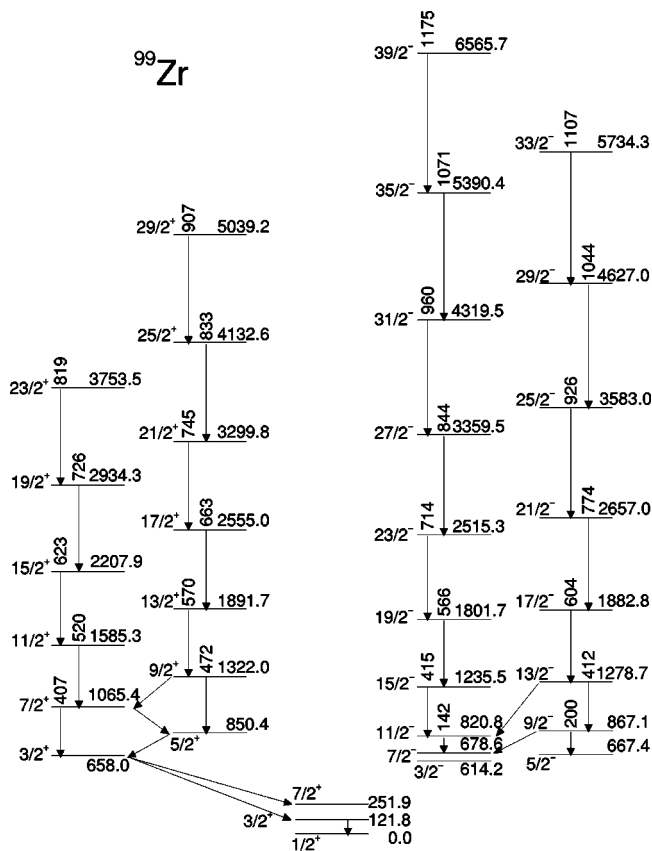


FIG. 9. Partial level scheme of ^{99}Zr with energies labeled in keV. The uncertainty on the transition energies is ≈ 1 keV.

from this mixing was identified to be the yrast structure for excited states with spin above 4^+ for both nuclei. Obviously, this scenario requires further study both experimentally and theoretically.

B. ^{97}Sr and ^{99}Zr

The spectroscopy of ^{97}Sr and ^{99}Zr , the $N=59$ isotones, also has been studied extensively in the past and the most

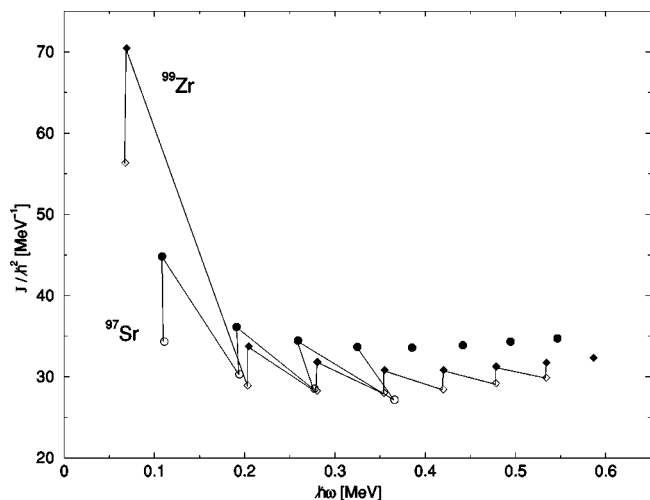


FIG. 10. Kinematic moment of inertia as a function of rotational frequency for the negative-parity yrast states having excitation energies above ≈ 600 keV in ^{97}Sr and ^{99}Zr .

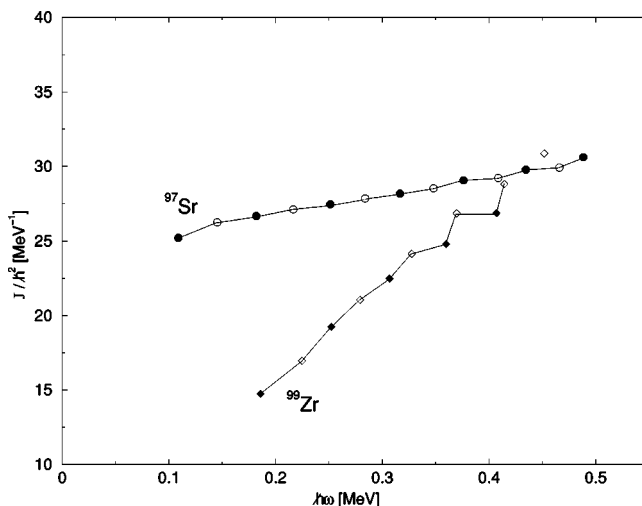


FIG. 11. Kinematic moment of inertia as a function of rotational frequency for the positive-parity yrast states having excitation energies above ≈ 600 keV in ^{97}Sr and ^{99}Zr .

recent results were reported in Ref. [16]. Partial level schemes of these nuclei deduced from the present work are shown in Figs. 8 and 9 for ^{97}Sr and ^{99}Zr , respectively. The excited states of ^{98}Sr have been extended from spin $27/2^-$ to spin $39/2^-$ at 6303.6 keV for the negative-parity band and

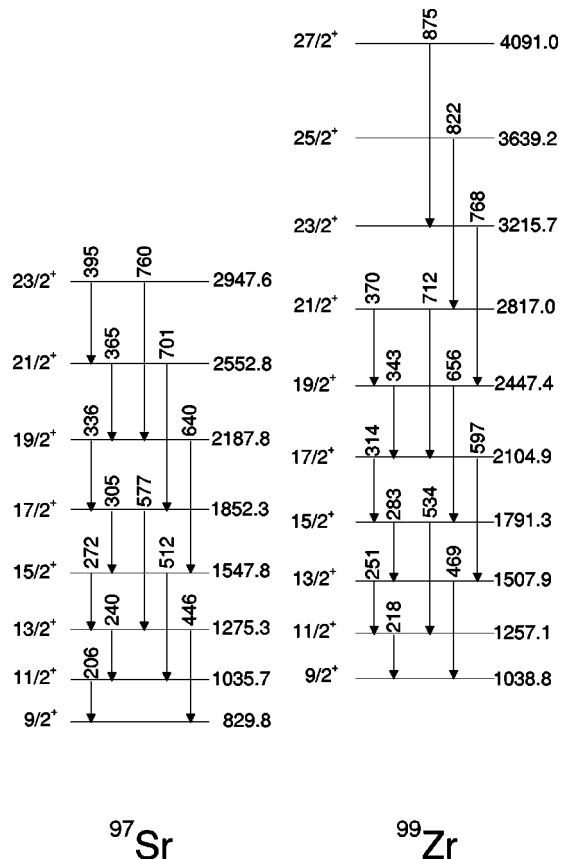


FIG. 12. Level schemes of rotational bands built on the $9/2^+[404]$ neutron configuration in ^{97}Sr and ^{99}Zr . Energies are in keV and the uncertainty on the transition energies is ≈ 1 keV.

TABLE II. Comparison of the $B(M1)/B(E2)$ ratio between the experimental values derived from the present work and the calculated ones using the rotational model with the single-particle configurations specified for both positive and negative states in ^{97}Sr and ^{99}Zr . Pure $M1$ was assumed for the $\Delta I=1$ transitions.

Initial state	E_x (keV)	E_γ (keV)		$B(M1)B(E2)(\mu_N^2/e^2b^2)$			
		$\Delta I=1$	$\Delta I=2$	Experiment	Calculation		
^{97}Sr							
Configuration							
					1/2 ⁻ [550]	3/2 ⁻ [541]	5/2 ⁻ [532]
9/2 ⁻	946.3	175.2	232.5	0.163(17)	0.123	0.54	1.69
^{99}Zr							
Configuration							
					1/2 ⁻ [550]	3/2 ⁻ [541]	5/2 ⁻ [532]
9/2 ⁻	867.1	188.5	199.7	0.047(3)	0.110	0.56	1.86
13/2 ⁻	1278.7	457.9	411.6	0.033(3)	0.104	0.47	1.10
Configuration							
					3/2 ⁺ [411]	3/2 ⁺ [422]	
7/2 ⁺	1065.4	215.0	407.4	0.57(4)	1.46	0.115	
9/2 ⁺	1322.0	256.6	471.6	0.62(4)	1.09	0.086	

from spin 21/2⁺ to spin 31/2⁺ at 4922.8 keV for the positive-parity band. For ^{99}Zr , the excited states have been extended from spin 27/2⁻ to spin 39/2⁻ at 6565.7 keV for the negative-parity band and from spin 21/2⁺ to spin 29/2⁺ at 5039.2 keV for the positive-parity band.

For the negative-parity band, the quadrupole deformation, β_2 , was determined to be 0.32 and 0.28 for ^{97}Sr and ^{99}Zr , respectively [16]. The moments of inertia for these bands, with the excitation energy above ≈ 600 keV, plotted as a function of rotational frequency are given in Fig. 10. A unique feature shown in this figure is that the moment of inertia is nearly constant for rotational frequency beyond ≈ 200 keV. The nonobservation of band crossing, which oc-

curs at the rotational frequency ≈ 500 keV for the Zr isotopes [22], implies the underlying single-particle configuration is related to $h_{11/2}$ neutron orbitals. However, the K quantum number cannot be determined uniquely from the comparison of $B(M1)/B(E2)$ ratios between the data and the calculated values for various single-particle configurations, which are listed in Table II. The calculated values were obtained using the g_K derived from Ref. [39] and $g_R=0.2\mu_N$ [40]. The experimental values were obtained from the measured γ -ray branching ratios between the $\Delta I=1$ and $\Delta I=2$ transitions, which are listed in Table I. One possible explanation for the observed $B(M1)/B(E2)$ ratios is configuration mixing among the $h_{11/2}$ orbitals due to the Coriolis coupling. Note that since the K quantum number cannot be determined uniquely, pure $M1$ was assumed for the $\Delta I=1$ transitions in deriving the experimental $B(M1)/B(E2)$ ratios and $K=3/2$ was assumed for calculating the moments of inertia, shown in Fig. 10.

For the positive-parity band, the moments of inertia for states with excitation energies above ≈ 600 keV, plotted as a function of rotational frequency, are shown in Fig. 11 for both nuclei. In contrast to the similar moments of inertia for the negative-parity bands, the moments of inertia for the positive-parity bands in ^{97}Sr and ^{99}Zr have a different dependence on rotational frequency. This is a consequence of the difference in the underlying single-particle configuration. It is likely that the positive-parity band in ^{99}Zr has significant components of both the 3/2⁺[411] and 3/2⁺[422] neutron orbitals as derived from the observed $B(M1)/B(E2)$ ratios, which are listed in Table II. These neutron orbitals cross each other as the quadrupole deformation increases and will have considerable mixing near $\beta_2 \approx 0.20$ according to the calculation given by, for example, Ref. [41]. The difference in

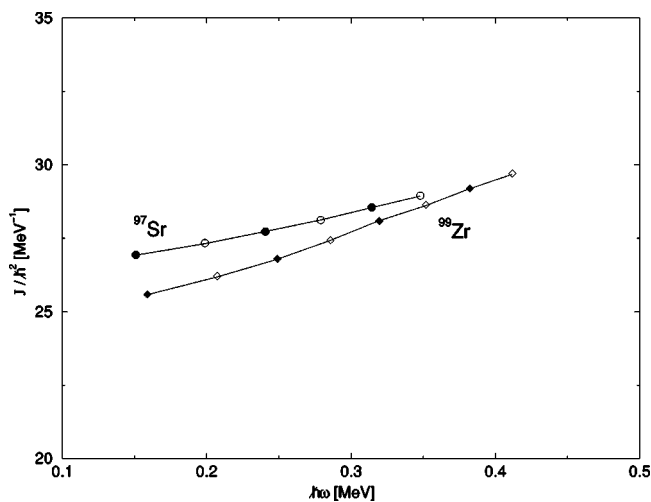


FIG. 13. Kinematic moment of inertia as a function of rotational frequency for the $\nu 9/2^+[404]$ rotational bands in ^{97}Sr and ^{99}Zr .

appearance of the moments of inertia for the positive-parity bands between these isotones may be a manifestation of a difference in the quadrupole deformation, which results in a different underlying single-particle composition of these neutron orbitals.

A strongly deformed band built on the $K^\pi=9/2^+$ isomer with an excitation energy at 1038.8 keV in ^{99}Zr has been reported recently [42]. This isomer corresponds to the $9/2^+[404]$ neutron excitation with $T_{1/2}=54(10)$ ns. A similar band has been reported for ^{97}Sr [43]. The $9/2^+$ isomer has an excitation energy at 829.8 keV with $T_{1/2}=265(27)$ ns. These isomer bands remain rather unmixed and have a quadrupole deformation, β_2 , near 0.4 [42,43]. Both bands were observed in this work and their level schemes are given in Fig. 12. Their moments of inertia plotted as a function of rotational frequency are shown in Fig. 13. The excited states have been extended from spin $17/2^+$ to spin $23/2^+$ at 2947.6 keV for ^{97}Sr and from spin $17/2^+$ to spin $27/2^+$ at 4091.0 keV for ^{99}Zr . The moment of inertia has a very similar appearance for these two isomer bands and increases slightly as the rotational frequency increases.

IV. SUMMARY

The spectroscopy of neutron-rich $^{96,97}\text{Sr}$ and $^{98,99}\text{Zr}$ has been studied by means of the prompt γ rays emitted from fission fragments, produced by the $^{238}\text{U}(\alpha, f)$ fusion-fission

reaction. With the increasing selectivity and sensitivity of the γ -ray spectroscopy for these nuclei studied using the γ -fission-fragment coincident technique, their level schemes were extended up to $\approx 20\hbar$, which, on average, is $\approx 6\hbar$ above the previously known spin and nearly double the known excitation energy. This extension allowed the observation of a sharp variation in the yrast structure of these nuclei despite the fact that their quadrupole deformation changes gradually. For example, the evolution of collective motion from vibrationlike to rotationlike with an increase in spin was observed for a moderately deformed shape in ^{96}Sr and ^{98}Zr . With an additional pair of neutrons, an increase in deformation occurs and well-defined rotational bands were observed in both ^{98}Sr and ^{100}Zr . The observed disparity in the dependence of the moment of inertia on the rotational frequency for the positive-parity band between ^{97}Sr and ^{99}Zr could be the result of deformation-dependent configuration mixing between the $3/2^+[411]$ and $3/2^+[422]$ neutron orbitals. The strongly deformed and relatively unmixed $9/2^+[404]$ band in the $N=59$ isotones has a rather weak dependence of the moment of inertia on the rotational frequency.

ACKNOWLEDGMENTS

The work by the Rochester group was funded by the National Science Foundation. The work at LBNL was supported in part by the U.S. DOE under Contract No. DE-AC03-76SF00098.

-
- [1] J. L. Wood, K. Heyde, W. Nazarewicz, M. Huyse, and P. Van Duppen, *Phys. Rep.* **215**, 101 (1992), and references therein.
 - [2] R. K. Sheline, I. Ragnarsson, and S. G. Nilsson, *Phys. Lett.* **41**, 115 (1972).
 - [3] T. A. Khan, W.-D. Lauppe, K. Sistemich, H. Lawin, and H. A. Selic, *Z. Phys. A* **284**, 313 (1978).
 - [4] F. K. Wohn, J. C. Hill, C. B. Howard, K. Sistemich, R. F. Petry, R. L. Gill, H. Mach, and A. Piotrowski, *Phys. Rev. C* **33**, 677 (1986).
 - [5] H. Mach, M. Moszynski, R. L. Gill, F. K. Wohn, J. A. Winger, J. C. Hill, G. Molnar, and K. Sistemich, *Phys. Lett. B* **230**, 21 (1989).
 - [6] H. Mach, M. Moszynski, R. L. Gill, G. Molnar, F. K. Wohn, J. A. Winger, and J. C. Hill, *Phys. Rev. C* **41**, 350 (1990).
 - [7] K. Heyde and R. A. Meyer, *Phys. Rev. C* **37**, 2170 (1988).
 - [8] J. L. Wood, E. F. Zganjar, C. De Coster, and K. Heyde, *Nucl. Phys.* **A651**, 323 (1999).
 - [9] C. Y. Wu, H. Hua, and D. Cline, *Phys. Lett. B* **541**, 59 (2002).
 - [10] C. Y. Wu, H. Hua, and D. Cline, *Phys. Rev. C* **68**, 034322 (2003).
 - [11] ISOLDE Collaboration, G. Lhersonneau, B. Pfeiffer, K.-L. Kratz, T. Enqvist, P. P. Jauho, A. Jokinen, J. Kantele, M. Leino, J. M. Parmonen, H. Penttila, and J. Aysto, *Phys. Rev. C* **49**, 1379 (1994).
 - [12] M. Buscher, R. F. Casten, R. L. Gill, R. Schuhmann, J. A. Wigner, H. Mach, M. Moszynski, and K. Sistemich, *Phys. Rev. C* **41**, 1115 (1990).
 - [13] H. Mach, F. K. Wohn, G. Molnar, K. Sistemich, J. C. Hill, M. Moszynski, R. L. Gill, W. Krips, and D. S. Brenner, *Nucl. Phys.* **A523**, 197 (1991).
 - [14] G. Lhersonneau, B. Pfeiffer, K.-L. Kratz, H. Ohm, K. Sistemich, S. Brant, and V. Par, *Z. Phys. A* **337**, 149 (1990).
 - [15] G. Lhersonneau, P. Dendooven, A. Honkanen, M. Huhta, P. M. Jones, R. Julin, S. Juutinen, M. Oinonen, H. Penttila, J. R. Persson, K. Perajarvi, A. Savelius, J. C. Wang, and J. Aysto, *Phys. Rev. C* **56**, 2445 (1997).
 - [16] W. Urban, J. L. Durell, A. G. Smith, W. R. Phillips, M. A. Jones, B. J. Varley, T. Rzaca-Urban, I. Ahmad, L. R. Morss, M. Bentaleb, and N. Schulz, *Nucl. Phys.* **A689**, 605 (2001).
 - [17] P. J. Nolan, F. A. Beck, and D. B. Fossan, *Annu. Rev. Nucl. Part. Sci.* **44**, 561 (1994).
 - [18] A. G. Smith *et al.*, *Phys. Rev. Lett.* **73**, 2540 (1994).
 - [19] M. W. Simon *et al.*, in *Proceedings of the International Conference on Fission and Properties of Neutron Rich Nuclei, Sanibel Island, FL*, edited by J. H. Hamilton and A. V. Ramayya (World Scientific, Singapore, 1998), p. 270.
 - [20] M. W. Simon, Ph.D. thesis, University of Rochester, 1999.
 - [21] M. W. Simon, D. Cline, C. Y. Wu, R. W. Gray, R. Teng, and C. Long, *Nucl. Instrum. Methods Phys. Res. A* **452**, 205 (2000).
 - [22] H. Hua, C. Y. Wu, D. Cline, A. B. Hayes, R. Teng, R. M. Clark, P. Fallon, A. Goergen, A. O. Macchiavelli, and K. Vetter, *Phys. Rev. C* **69**, 014317 (2004).
 - [23] J. H. Hamilton, A. V. Ramayya, S. J. Zhu, G. M. Ter-akopian, YU. TS. Oganessian, J. D. Cole, J. O. Rasmussen, and M. A.

- Stoyer, *Prog. Part. Nucl. Phys.* **35**, 635 (1995).
- [24] C. Y. Wu, H. Hua, D. Cline, A. B. Hayes, R. Teng, R. M. Clark, P. Fallon, A. Goergen, A. O. Macchiavelli, and K. Vetter, *Proceedings of the International Conference on Frontiers of Nuclear Structure, Berkeley, CA*, edited by P. Fallon and R. Clark (American Institute of Physics, New York, 2002), p. 408.
- [25] H. Hua, C. Y. Wu, D. Cline, A. B. Hayes, R. Teng, R. M. Clark, P. Fallon, A. Goergen, A. O. Macchiavelli, and K. Vetter, *Phys. Lett. B* **562**, 201 (2003).
- [26] C. Y. Wu, H. Hua, D. Cline, A. B. Hayes, R. Teng, R. M. Clark, P. Fallon, A. Goergen, A. O. Macchiavelli, and K. Vetter, *Proceedings of the Third International Conference on Fission and Properties of Neutron-Rich Nuclei, Sanibel Island, FL*, edited by J. H. Hamilton, A. V. Ramayya, and H. K. Carter (World Scientific, Singapore, 2003), p. 199.
- [27] J. Weber, H. Specht, E. Konechy, and D. Heunemann, *Nucl. Phys.* **A221**, 414 (1974).
- [28] K. Vetter *et al.*, *Phys. Rev. C* **58**, R2631 (1998).
- [29] C. Y. Wu, M. W. Simon, D. Cline, G. A. Davis, R. Teng, A. O. Macchiavelli, and K. Vetter, *Phys. Rev. C* **64**, 064317 (2001).
- [30] A. B. Hayes *et al.*, *Phys. Rev. Lett.* **89**, 242501 (2002).
- [31] C. Y. Wu, D. Cline, M. W. Simon, R. Teng, K. Vetter, M. P. Carpenter, R. V. F. Janssens, and I. Wiedenhover, *Phys. Rev. C* **68**, 044305 (2003).
- [32] P. H. Regan *et al.*, *Phys. Rev. C* **68**, 044313 (2003).
- [33] J. J. Valiente-Dobon *et al.*, *Phys. Rev. C* **69**, 024316 (2004).
- [34] S. Raman, C. H. Malarkey, W. T. Milner, C. W. Nestor, Jr., and P. H. Stelson, *At. Data Nucl. Data Tables* **36**, 1 (1987).
- [35] P. H. Regan *et al.*, *Phys. Rev. Lett.* **90**, 152502 (2003).
- [36] L. K. Peker, *Nucl. Data Sheets* **68**, 165 (1993).
- [37] B. Singh and Z. Hu, *Nucl. Data Sheets* **98**, 335 (2003).
- [38] J. Skalski, P. H. Heenen, and P. Bonche, *Nucl. Phys.* **A559**, 221 (1993).
- [39] E. Browne and F. R. Femenia, *Nucl. Data Tables* **10**, 81 (1971).
- [40] H. Mach, F. K. Wohn, M. Moszynski, R. L. Gill, and R. F. Casten, *Phys. Rev. C* **41**, 1141 (1990).
- [41] J. Skalski, S. Mizutori, and W. Nazarewicz, *Nucl. Phys.* **A617**, 282 (1997).
- [42] W. Urban, J. A. Pinston, T. Rzaca-Urban, A. Zlomaniec, G. Simpson, J. L. Durell, W. R. Phillips, A. G. Smith, M. A. Jones, B. J. Varley, I. Ahmad, and N. Schulz, *Eur. Phys. J. A* **16**, 11 (2003).
- [43] J. K. Hwang *et al.*, *Phys. Rev. C* **67**, 054304 (2003).